Indian Journal of Chemistry
Vol. 65, July 2026, pp. 680-690
DOI: 10.56042/ijc.v65i7.14794

Chelating molecular imaging probe amino polycarboxylic acid-manganese (II) complexes: As potent photoluminescent materials for imaging

Amutha Selvi M*, Sivasankari J, Merlin Vinoliya E&Nandini B

Department of Chemistry, Avinashilingam Institute for Home Science and Higher Education for Women, Coimbatore 641 043, Tamil Nadu, India

E-mail: amuthaselvi_chem@avinuty.ac.in

Received 1 November 2024; accepted (revised) 21 July 2026

The most used gadolinium and manganese-based contrast agents improve the visibility of internal cell body structures in MRI. To overcome the nephrogenic systemic fibrosis (NSF) related to renal impairment, we are in the race to find safer MRI contrast agents. The utilization of some paramagnetic transition metal ions, Mn^{2+} and Fe^{3+} that may effectively relax the water protons is a potential strategy for developing substitute contrast agents for Gd^{3+}chelates and these metals are less harmful than Gd^{3+}. This investigation concentrates on synthesis of DTPA and EDTA-based manganese complexes with two different poly amino carboxylic acids to enhance as potential contrast agents with further studies. DTPA/EDTA anhydrides and respective amino substituted ligands have been prepared under nitrogen atmosphere and complexes have been prepared by reflux method at *p*H 8.4 using 1N $NaHCO_3$ solution which has been characterized by UV-Vis, FTIR, ^{1}H NMR, EPR, and TGA studies. FT-IR analysis shows 510 cm^{-1} M-O bond and shifting of the ranges observed on comparing ligand and metal studies which confirms the metal complex formation. 10.5 – 10.6 ppm for COOH group and 5.8 – 5.9 ppm for N-H group confirm the formation of poly amino carboxylic acid ligands with DTPA/EDTA. Nuclear spin I=5/2 reveals the $3d^5$ electronic configuration for Mn. The Mn complexes have shown good thermal stability, and EDTA complexes have good bacterial-resistant activity. Both DTPA/EDTA complexes have good fluorescence activities. The manganese-based complexes show good resistance against both Gram positive and Gram negative bacteria which are well-suited to the human body, with excellent emissions of complexes that may lead to further studies for imaging agents.

Keywords: Contrast agents, Photoluminescent materials, Paramagnetic complexes, Molecular imaging probe

The most used gadolinium and manganese-based contrast agents improve the visibility of internal cell body structures in magnetic resonance imaging. The MRI contrast agents (CA's) alters the relaxation times (shortening the T1 relaxation time) of atoms within body tissues where they are present after oral or intravenous administration[1–5]. To overcome Nephrogenic systemic fibrosis (NSF), related to renal impairment, we are in the race to find safer MRI contrast agents. The utilization of some paramagnetic transition metal ions, Mn^{2+} and Fe^{3+} that may effectively relax the water protons is a potential strategy for developing substitute contrast agents for Gd^{3+} chelates and these metals are less harmful than Gd^{3+}. However, due to their lower magnetic moments, fewer unpaired electron and slightly faster electronic relaxation durations than Gd^{3+}, its medical use is proscribed because of its toxicity and less desirable for MRI applications.

Presently, Mn^{2+} - dipyridoxyldiphosphate, Mn-$(DPDP)^{3-}$ is the only Mn^{2+} based CA available for use in liver imaging[6]. It has been demonstrated that $[Mn(DPDP)]^{3-}$ partially dechelates in plasma, with the Mn^{2+} ion being swiftly absorbed by hepatocytes, pancreatic tissue, and cardiomyocytes. The potential and difficulty of employing Mn^{2+} are both shown by $[Mn(DPDP)]^{3-}$. In addition to highlighting the great lability of the Mn^{2+} ion and the difficulty of creating a stable Mn-chelate, $[Mn(DPDP)]^{3-}$ produced an excellent picture contrast that showed the effectiveness of an Mn-based method. The negatively charged oxygen and nitrogen donor atoms are preferred by the "hard" Mn^{2+} ion. As a result of their symmetrical d5 electron configuration and lack of ligand field stabilization energy, most Mn^{2+} complexes follow the Irving Williams order of relative stability. Hence, among the divalent first-row transition metal high spin complexes, Mn^{2+} complexes have the lowest stability. It makes sense to generate chelators that allow stable Mn^{2+} complexes to be used in the MR imaging applications as Gd-based probes are, amongst them are bifunctional Mn^{2+} chelators for molecular MR applications and tiny, hydrophilic complexes that are

useful for tissue perfusion characterization, angiography, and lesion identification[7]. This also demonstrates the difficulty in creating Mn^{2+} based MRI contrast agents. The Mn^{2+} ion typically has a coordination number of 6 or 7 and complexes with the highest stability are those generated with ligands that have a corresponding number of donor atoms[8]. Fast water exchange, acceptable T1 relaxivities, the possibility of undergoing redox chemistry *in vivo*, and other characteristics of high spin Mn^{2+} complexes make them appealing as MRI agents.

It is beneficial to bind Mn(II) ions to ideal ligand like Ethylene diamine tetra acetic acid(EDTA), Dipyridoxy diphosphate(DPDP), Diethyelenetriaminepentaacetic acid(DTPA), Phenylpentadecanoic acid(PPDA), Benzothiazole aniline(BTA), *etc*.[9] (Y.Huang *et al*., 2011). Mn(II)-DTPA CA has high chelation efficiency and the release of free Mn (II) ions into the blood is also low. Hence development of stable and secured Mn(II) based potential MRI contrast agents has become a ceaseless quest. Mn-DTPA CA has significant applications in MRI techniques.

When we compare the relaxivities of Mn-based CA's, MNP-PEG-Mn is much higher than that of Gadodiamide[10,11] (Xiaodong Li *et al*., 2020) (Mauro Botta *et al*., 2019). According to Y. Huang *et al*., (2011), it is advantageous to bind Mn (II) ions to optimal ligands such as Benzothiazole aniline (BTA), PhenylpentadecanoicAcid(PPDA), DiethyelenetriaminePentaAceticAcid(DTPA), Dipyridoxy diphosphate (DPDP), and Ethylene Diamine Tetra Acetic Acid (EDTA). High chelation effectiveness and minimal leakage of free Mn (II) ions into the circulation are both characteristics of Mn (II)-DTPA contrast agent. Therefore, the search for potentially useful Mn(II)-based MRI contrast agents has never ended. The MRI technology uses the Mn-DTPA contrast agent extensively. This work concentrates on preparing DTPA and EDTA-based manganese complexes which can be further studied to be used as a contrast agent.

Experimental Section

Chemicals

Chemicals like DTPA, Disodium salt of EDTA, 4-amino benzoic acid and 6-amino naphthoic acid were purchased from SRL Chemicals and Sigma Aldrich in 99% purity. Solvents like Dimethyl formamide, Triethylamine, Pyridine, and Acetic anhydride were commercially available and used without any further purification.

Physical Measurements

IR spectra were obtained from Shimadzu IR spectrometer. NMR spectra were recorded in a BRUKER modern 400 MHz instrument with TMS as an internal standard. EPR spectrum of complex was recorded using JOEL Model JES FA200. TGA of complexes were determined using TG/DTA-EXSTAR/6300. Fluorescent spectra of compounds were recorded using Agilent Cary Eclipse fluorescence Spectrometer. Anti-bacterial studies of the compounds were done by Kirby-Bauer method using bacteria namely *E.coli* and *Staphylococccus aureus* with reference to Rifampicin and Ampicillin as standards.

Anti-Bacterial Test (Kirby-Bauer method)

Growth Method

The antibacterial activity of the amino polycarboxylic complexes was evaluated based on the growth method mentioned in[23] using Gram positive *Staphylococcusaureus*and Gram negative *E. coli* bacterial strains. The bacterial broth suspensions contained 1 to 2×10^8 CFU/mL for each prepared bacteria. Petri dishes were inoculated by agar over the entire plate and left for 3-5 minutes to allow excess moisture absorption, media punctured, and 6 mm well filled with a 20 µl sample. To obtain complete diffusion and zone of inhibition the plates were placed inversely and examined the well after 24 h incubation at 37°C.

Synthesis

Stage I: Preparation of bis anhydride

In a double neck round bottom flask added DTPA/EDTA mixture, acetic anhydride, pyridine and were heated in a magnetic stirrer at 80°C for 18 hours under nitrogen atmosphere. The mixture was cooled to RT, and filtered, and the resulting solid was washed with acetic anhydride and diethyl ether. It was then placed in an oven to dry and the yield of the dried product was noted. Since EDTA is available in the form of Disodium salt, prior to this step it is converted to H4EDTA. This is done according to the method followed in the literature.

Stage II: Preparation of Ligand

DTPA/EDTA bis anhydride was dissolved in DMF and triethylamine was mixed under nitrogen atmosphere in a double neck round bottom flask. 4-amino benzoic acid/6-amino naphthoic acid was dissolved in DMF and added to it. *p*H of the solution was maintained at 8. Triethylamine was added to

maintain the *p*H of the mixture. The reaction was heated at 40°C with stirring for 7 hours. The solution was reduced to half to remove excess solvent and kept for drying to obtain product. The yield of the product was noted.

Stage III: Preparation of Complex

Manganese (II) chloride and the prepared ligand of DTPA/EDTA with 4-amino benzoic acid/6-amino naphthoic acid were taken in a round bottom flask. The *p*H was maintained at 8.4 using 1N $NaHCO_3$ solution and dissolved. To the solution added 2 mL of 1N HCl to maintain the *p*H of the resulting solution and kept in water bath at 70°C for 6 hours. Then the resulting solution was subjected to direct flame for 2 minutes in a wavering manner and allowed to cool. The excess solvent was evaporated and complex was formed. The yield was noted.

Results and Discussion

UV-Vis Spectroscopy

The electronic spectra of DTPA compounds showed an absorption band in the range 240-270 nm which may be attributed to $\pi \rightarrow \pi^*$ transition of the aromatic moiety of ligands**.** This absorption band remained unaltered in their complexes. A shoulder around 320-400 nm may be due to the ligand to metal charge transfer (LMCT) transition. The weak absorption at 550 nm may be assigned to the spin allowed d-d transition[12]. The λ_{max} of EDTA-based ligands show good absorption at 290nm – 310 nm. Complex of 6-amino naphthoic acids showed a weak $n \rightarrow \pi^*$ transition showing good absorption near 310 nm. The complexes Mn-EDTABis-4ABA and Mn-EDTABis-6ANA showed a hypsochromic shift compared to the ligands.

Fourier Transform Infrared Spectra

In the IR spectrum of the EDTA-Bisanhydride and DTPA-Bisanhydride showed a peak at 1749 and 1771 cm^{-1} corresponding to symmetric C=O stretch of anhydride. A peak at 1255 cm^{-1} and 1342 cm^{-1} corresponded to C-O stretch of the ligands EDTA-Bisanhydride and DTPA-Bisanhydride. A peak range from 1062 – 1110 cm^{-1} and 930 – 949 cm^{-1} corresponded to C-N stretch and O-H bend respectively[13].The carboxylic acid group resides at 1689 cm^{-1}.

In the IR spectrum (Fig. 1) of the ligand DTPABis-4ABA, the strong band at 1689 cm^{-1} can be attributed to the absorption of carboxyl groups υ(C=O). The three bands at 1627, 1527 and 1396 cm^{-1} could be assigned to absorptions of amide respectively. In the band of wavelength 1620 cm^{-1} assigned to amide absorptions in DTPA Bis-6ANA, two weak bands at 2916 cm^{-1} revealed the O-H stretching of carboxylic acid, 1087 cm-1 exhibited the N-H stretching[14-18].

In the IR spectrum (Fig. 2) of EDTABis-4ABA, the strong band at 1658 cm^{-1} can be assigned to the absorption of carboxyl groups υ(C=O). The three bands at 1597, 1473 and 1396 cm^{-1} could be assigned to absorptions of amide respectively. In the band of wavelength 1620 cm^{-1} assigned to amide absorptions in EDTABis-6ANA, two weak bands at 2924 cm^{-1} revealed the O-H stretching of carboxylic acid, 1103 cm^{-1} exhibited the N-H stretching.

In the IR spectrum of the metal complex Mn-DTPABis-4ABA the peaks at 1627, 1527, and 1396 cm^{-1} disappeared and strong absorption peaks at 1550 cm^{-1} and 1404 cm^{-1} were present. This indicated the formation of the complex. The metal-oxygen bond at 509 cm^{-1} was present in the IR spectra of MnDTPABis-4ABA. In the band of wavelength 1620 cm^{-1} assigned to amide absorptions in DTPABis-6ANA, two weak bands at 2916 cm^{-1} revealed the O-H stretching of carboxylic acid, and 1087 cm^{-1} exhibited the N-H stretching.

In the IR spectrum of the metal complex Mn-EDTABis-4ABA the peaks at 1627, 1527, and 1396 cm^{-1} disappeared and strong absorption peaks at 1550 cm^{-1} and 1404 cm^{-1} were present. This indicated the formation of the complex. The metal-oxygen bond at 510 cm^{-1} was present in the IR spectra of MnEDTABis-4ABA. In the band of wavelength 1620 cm^{-1} assigned to amide absorptions in EDTABis-6ANA, two weak bands at 2931 cm^{-1} revealed the O-H stretching of carboxylic acid, and 1149 cm^{-1} exhibited the N-H stretching. Both the ligands and their complexes vibrational frequencies have been listed in (Table 1).

NMR spectra of ligands DTPA Bis-4ABA and DTPA Bis-6ANA

A peak at δ=2.5 ppm and a peak at δ=2.6 ppm corresponds to DMSO d6 solvent of DTPABis-4ABA and DTPABis-6ANA respectively have shown in (Fig. 3). A peak at δ=7.6(d) ppm corresponds to the four aromatic protons of 4-amino benzoic acid and the peak at δ=7.8(d) ppm corresponds to the six aromatic

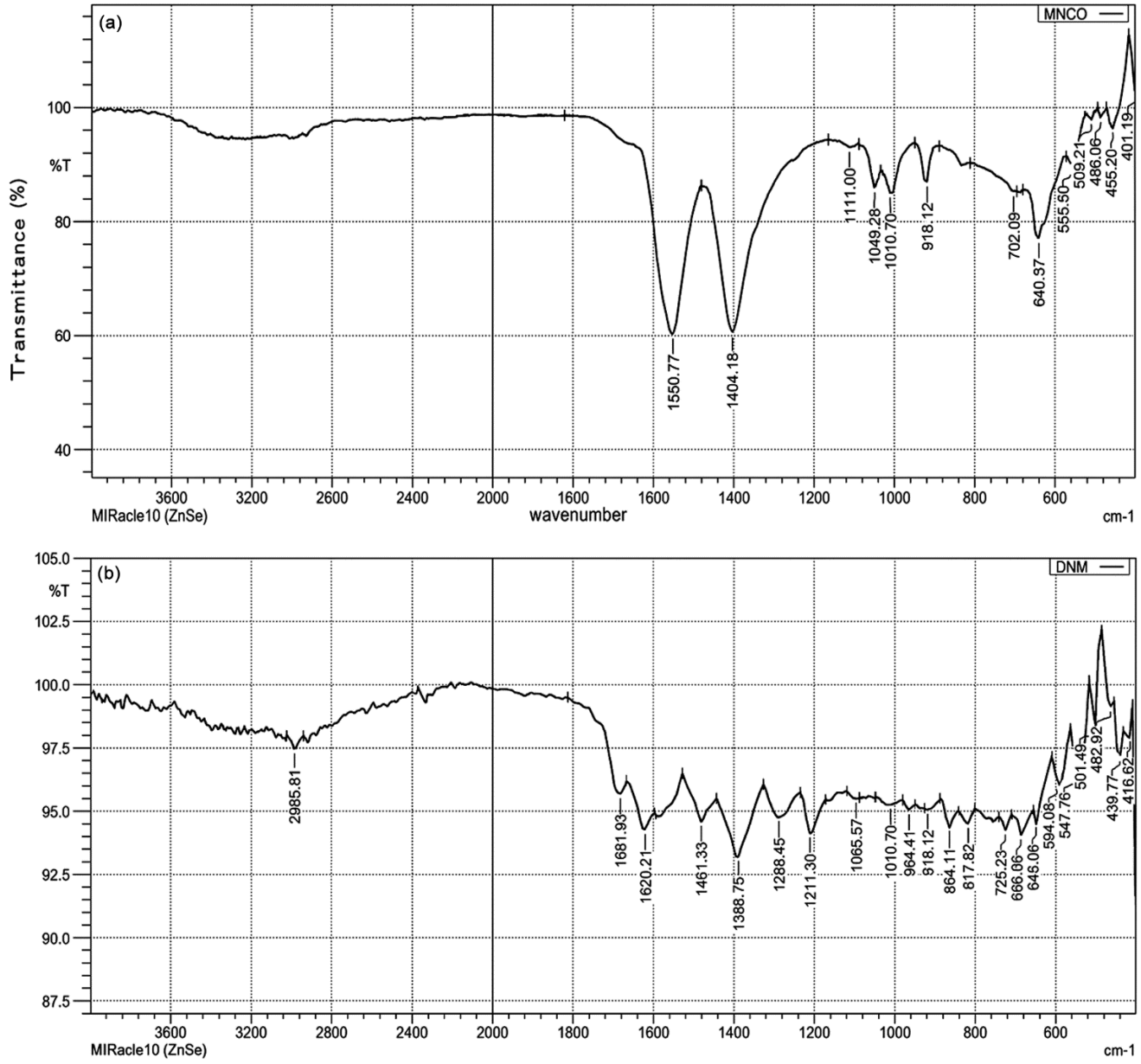

Fig. 1 — IR spectrum of Mn-DTPABis-4ABA and Mn-DTPABis-6ANA

protons of 6-amino naphthoic acid. A triplet appearing at the range of δ=2.9-3-3(t)ppm corresponds to the four methylene protons of N-CH2-CH2-N-group in DTPABis. ^{1}H NMR showed a sharp singlet at around δ=3.4-3.7 ppm(s) corresponding to the four methylene protons of N-CH2-C=O, which showed the chemical equivalence of methylene groups in DTPABis-4ABA and DTPABis-6ANA respectively. A peak at 5.8 ppm corresponds to amine protons and a singlet at 10.5 ppm corresponds to carboxylic acid.

NMR spectra of ligands EDTA Bis-4ABA and EDTA Bis-6ANA

A peak at δ=2.7 ppm and a peak at δ=2.6 ppm corresponds to DMSO d6 solvent of EDTABis-4ABA and EDTABis-6ANA respectively have displayed in (Fig. 4). A peak at δ=7.8(d) ppm corresponds to the four aromatic protons of 4-amino benzoic acid and the peak at δ=7.7(d) ppm corresponds to the six aromatic protons of 6-amino naphthoic acid. A triplet appearing at the range of δ=2.83(t)ppm corresponds to the four methylene protons of N-CH2-CH2-N-group

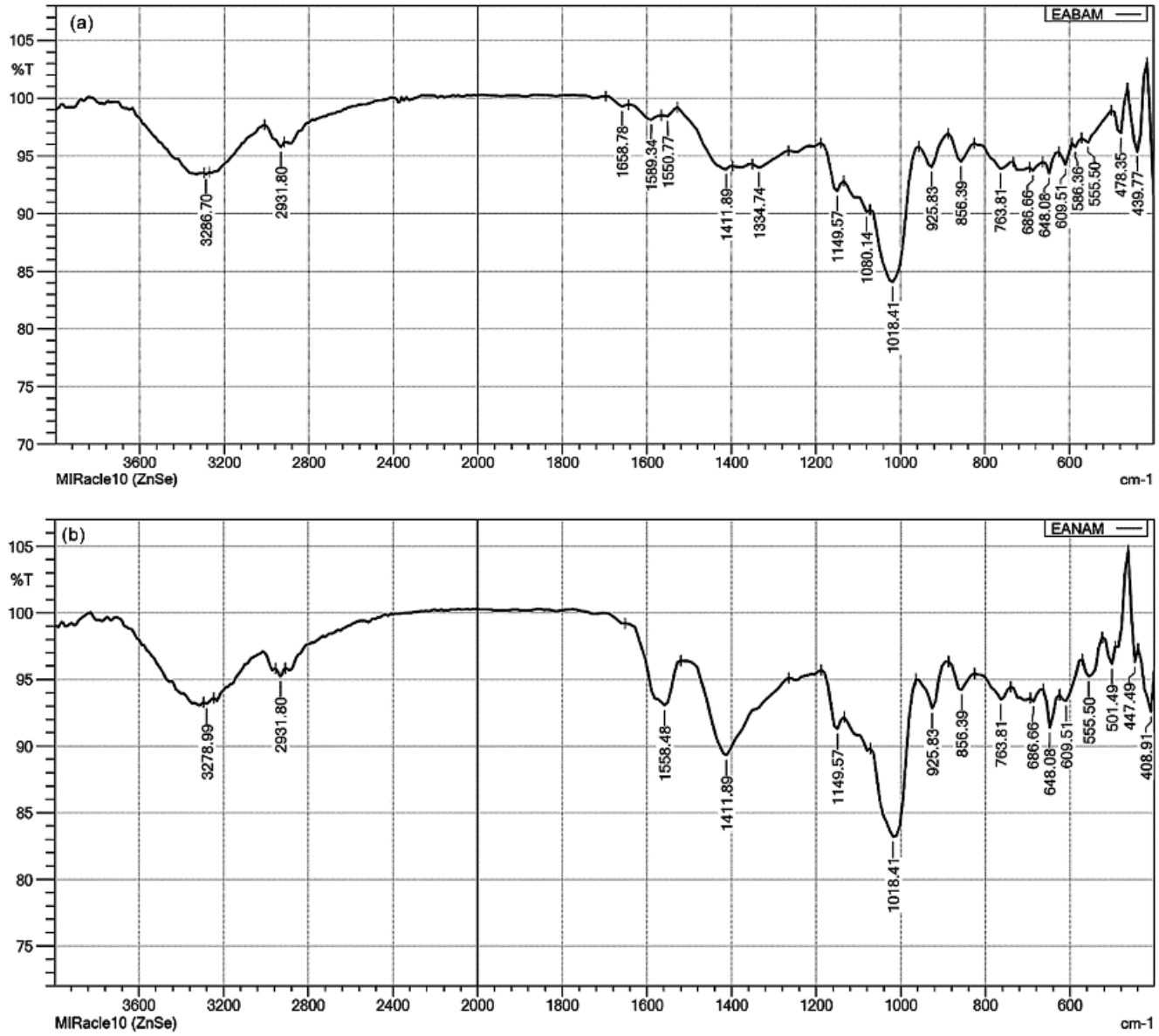

Fig. 2 — IR spectrum of Mn-EDTABis-4ABA and Mn-EDTABis-6ANA

Table 1 — Vibrational frequencies of ligands and complexes

Compd	cm^{-1}				
	υ(C=O) anhydride	υ(C-N)	υ(C=O)carboxyl	υ(C-N)amide	υ(Mn-O)
DTPABis	1771	1110	1689	1087	–
EDTABis	1749	1062	1658	1056	–
DTPABis-4ABA	–	1110	1689	1087	–
EDTABis-4ABA	–	1062	1658	1056	–
DTPABis-6ANA	–	1110	1692	1087	–
EDTABis-6ANA	–	1062	1658	1056	–
Mn-DTPABis-4ABA	–	1110	1689	1087	509
Mn-EDTABis-4ABA	–	1062	1658	1056	510
Mn-DTPABis-6ANA	–	1110	1692	1087	501
Mn-EDTABis-6ANA	–	1062	1658	1056	501

in EDTA Bis. ^{1}H NMR showed a sharp singlet at around δ=3.5ppm(s) corresponding to the four methylene protons of N-CH2-C=O, which showed the chemical equivalence of methylene groups in EDTABis-4ABA and EDTABis-6ANA respectively. A peak at 5.8 and 5.9 ppm corresponds to amine protons[19]. In Table 2 peaks of the functional groups in DTPA and EDTA ligands have been listed.

EPR spectrum of DTPA Bis-6ANA

The effective g value of 2.04 indicated that dipolar interactions between manganese ions are present. This is because Mn (II) ions have a $3d^5$ electronic configuration for the ^{55}Mn nucleus, with a nuclear spin of I=5/2. As a result, the EPR spectrum of the Mn (II) complex (Fig. 5) at ambient temperature exhibits a characteristic six-line hyperfine splitting. On the contrary, if the symmetry around the Mn (II) ion is distorted due to complexation, hence resonances become anisotropic, and a randomly oriented sample may show a broad line. The broad signal observed in this study implies that the complex's symmetry around the Mn (II) ion is distorted.

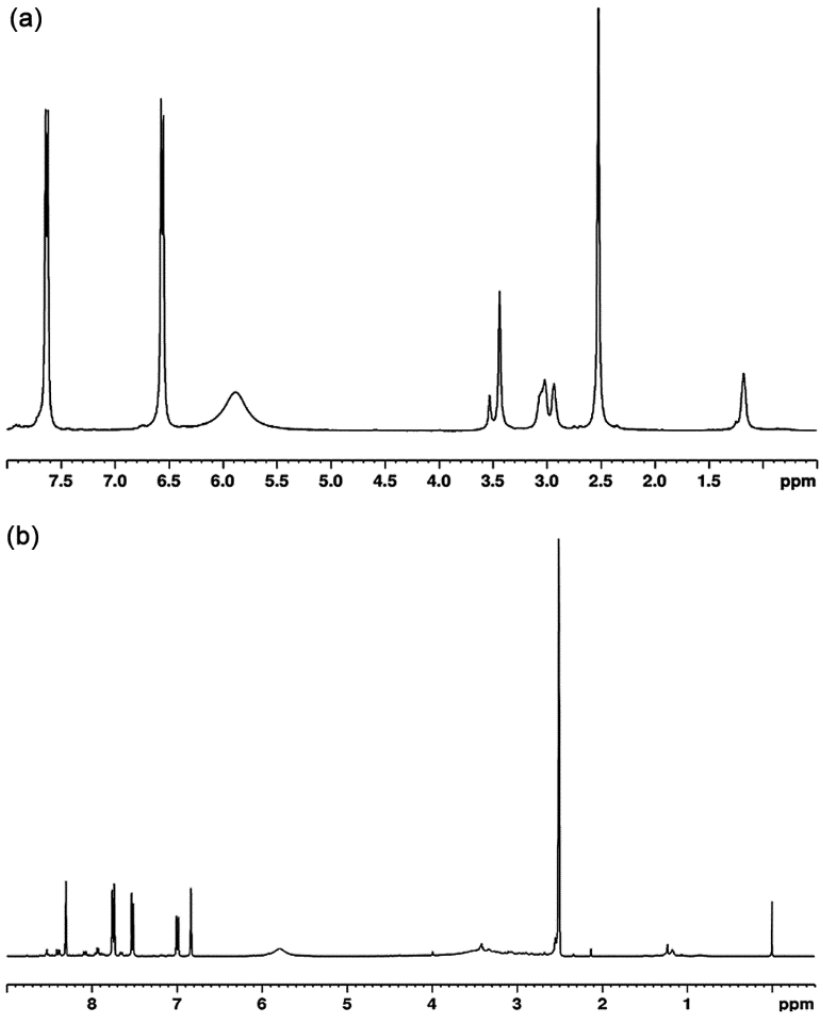

Fig. 3 — ^{1}H NMR of DTPABis-4ABA and DTPABis-6ANA

Table 2 — NMR peaks of ligands

Compd	–N*H*	–COO*H*	Ar-*H*	N-CH_2-C=O	N-CH_2-CH_2-N
EDTABis-4ABA	5.9	–	7.8	3.5	2.8
EDTABis-6ANA	5.8	10.6	7.7	3.4	2.9
DTPABis-4ABA	5.8	10.5	7.6	3.4	2.9
DTPABis-6ANA	5.8	10.6	7.8	3.7	3.3

Thermo Gravimetric Studies

Thermo Gravimetric Analysis (TGA) provides detailed information about the decomposition temperature of the analyte at various temperatures. TGA was taken for MnDTPABis-6ANA and MnEDTABis-4ABA as shown in (Fig. 6).

For MnDTPABis-6ANA, at a temperature 90°C, there is a slight weight loss due to the loss of water molecules. The weight loss at 110°C corresponds to sodium bicarbonate. At 320°C the weight loss is due to degradation of 6-amino naphthoic acid. The weight loss at 470°C is due to loss of DTPA molecule. After 650°C the metal decomposes as metal oxide.

For MnEDTABis-4ABA, at temperature 90°C there is a slight weight loss due to loss of water molecules. The weight loss at 110°C corresponds to sodium bicarbonate. The weight loss at 360°C corresponds to loss of 4-amino benzoic acid. At 450°C the weight loss is due to the decomposition of EDTA. After 650°C the metal decomposes as metal oxide.

Fluorescence Spectroscopy

Photoluminescence measurements allow us to study the emission properties of complexes. Excitation of the ligand 4-aminobenzoic acid at 278 and 378 nm resulted in an emission maximum at 350 and 450nm. The ligand 6-amino naphthoic acid excitation at 278 and 345nm resulted in an emission maximum at 420 and 420nm[20]. Similarly, DTPA complex with 4-aminobenzoic acid also exhibited emission shift from 248 and 305 to 410nm. The complex with 6-amino naphthoic acid also exhibited emission shift from 243 and 302 to 420 and 410 nm. In EDTA complexes, ligands EDTA Bis-4ABA and EDTABis-6ANA showed good fluorescence intensity at 353nm and 421nm respectively. The complex MnEDTABis-6ANA showed the maximum intensity at 411nm. Comparing the fluorescence activity of Gd-DTPA complexes, Mn–DTPA Bisanhydride complexes showed good fluorescence emission. Emission wavelength of commercial contrast agent

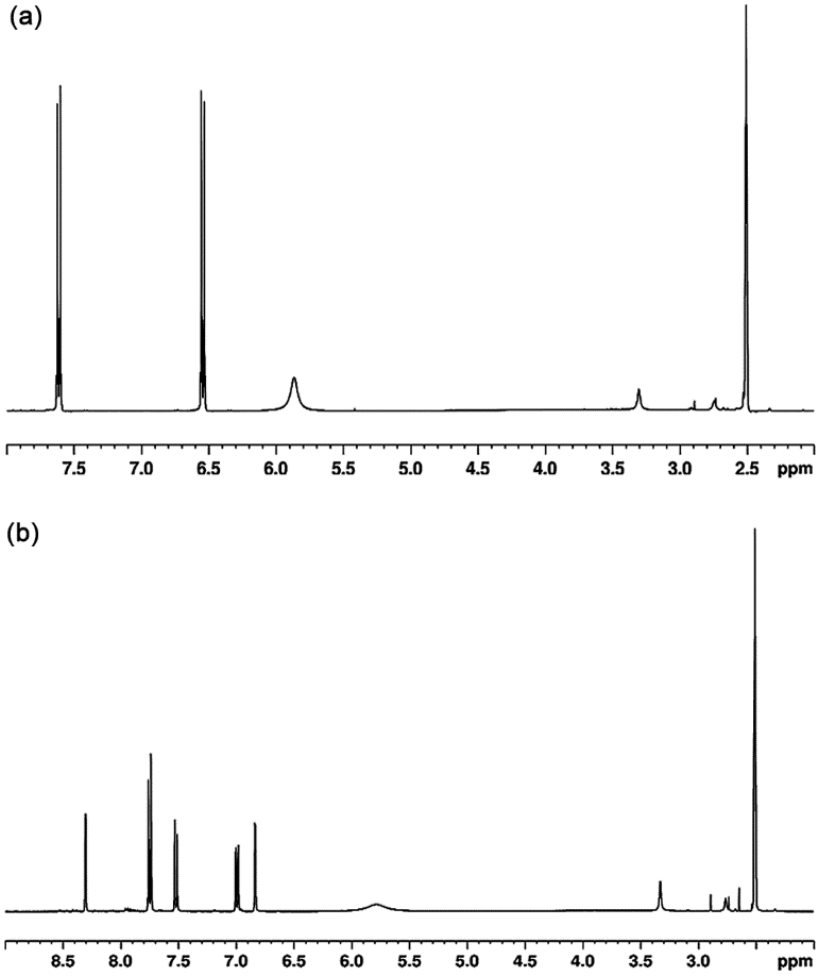

Fig. 4 — ^{1}H NMR of EDTA Bis-4ABA and EDTA Bis-6ANA

Gd-DTPA was at 305 nm (Ref. 21) due to f–f transition of central Gd^{3+}, whereas the emission wavelength of the prepared Mn – DTPA bisanhydride complexes exhibited at 410 nm. This red shift might be due to the increased π-conjugation because of the formation of C-N bond based on aromatic group of DTPA bis-anhydride with 4-aminobenzoic acid and 6-amino naphthoic acid. Compared to Mn – DTPAbis anhydride complexes, the range of fluorescent intensity of Gd-DTPA was low and nearly negligible. MnEDTABis-6ANA showed the maximum intensity out of all the complexes. These results suggest that

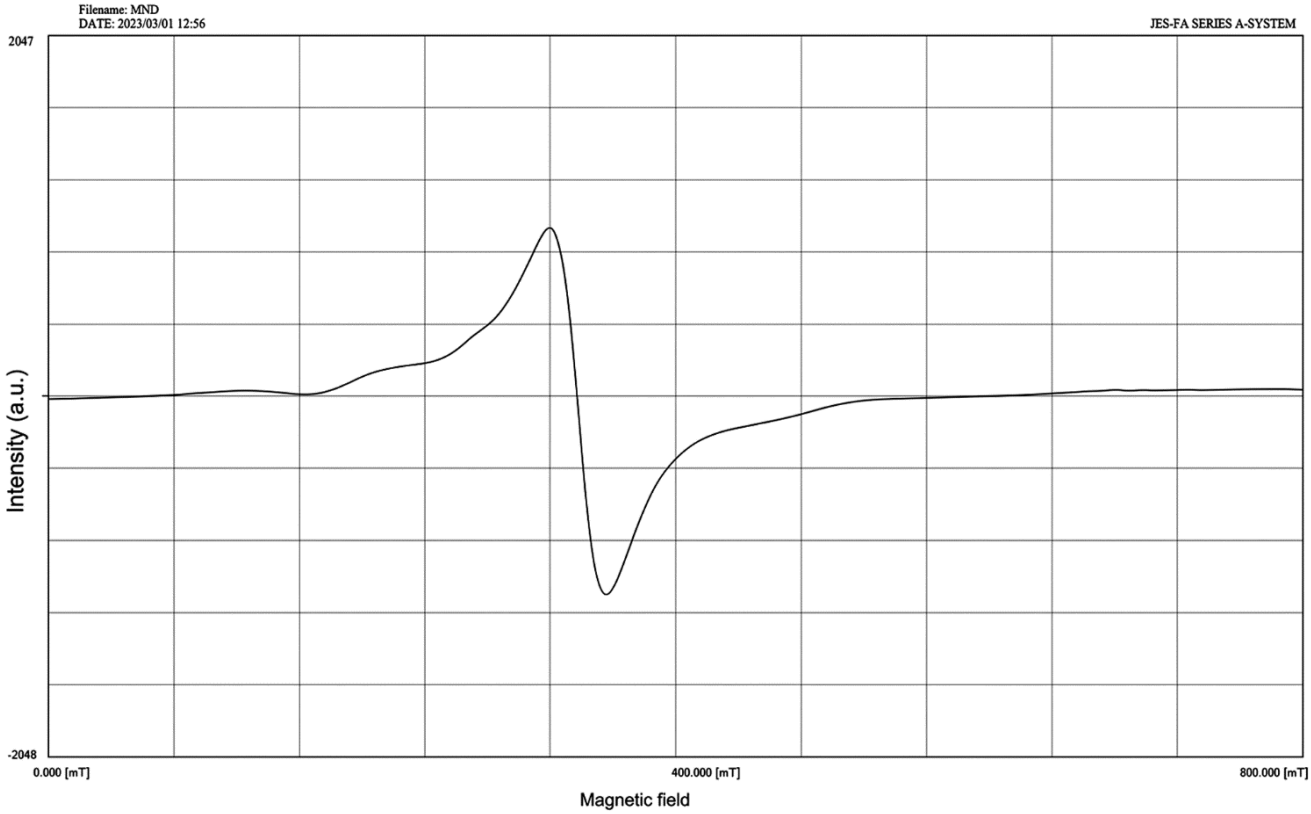

Fig. 5 — EPR spectrum of MnDTPA Bis-6ANA

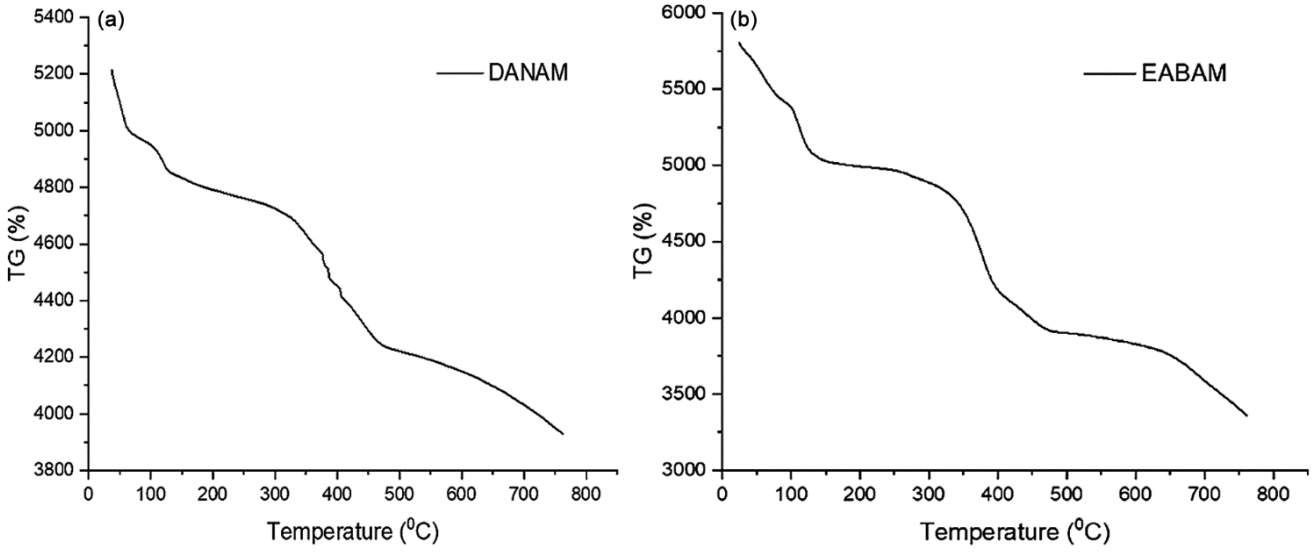

Fig. 6 — Thermogram of MnDTPABis-6ANA and MnEDTABis-4ABA

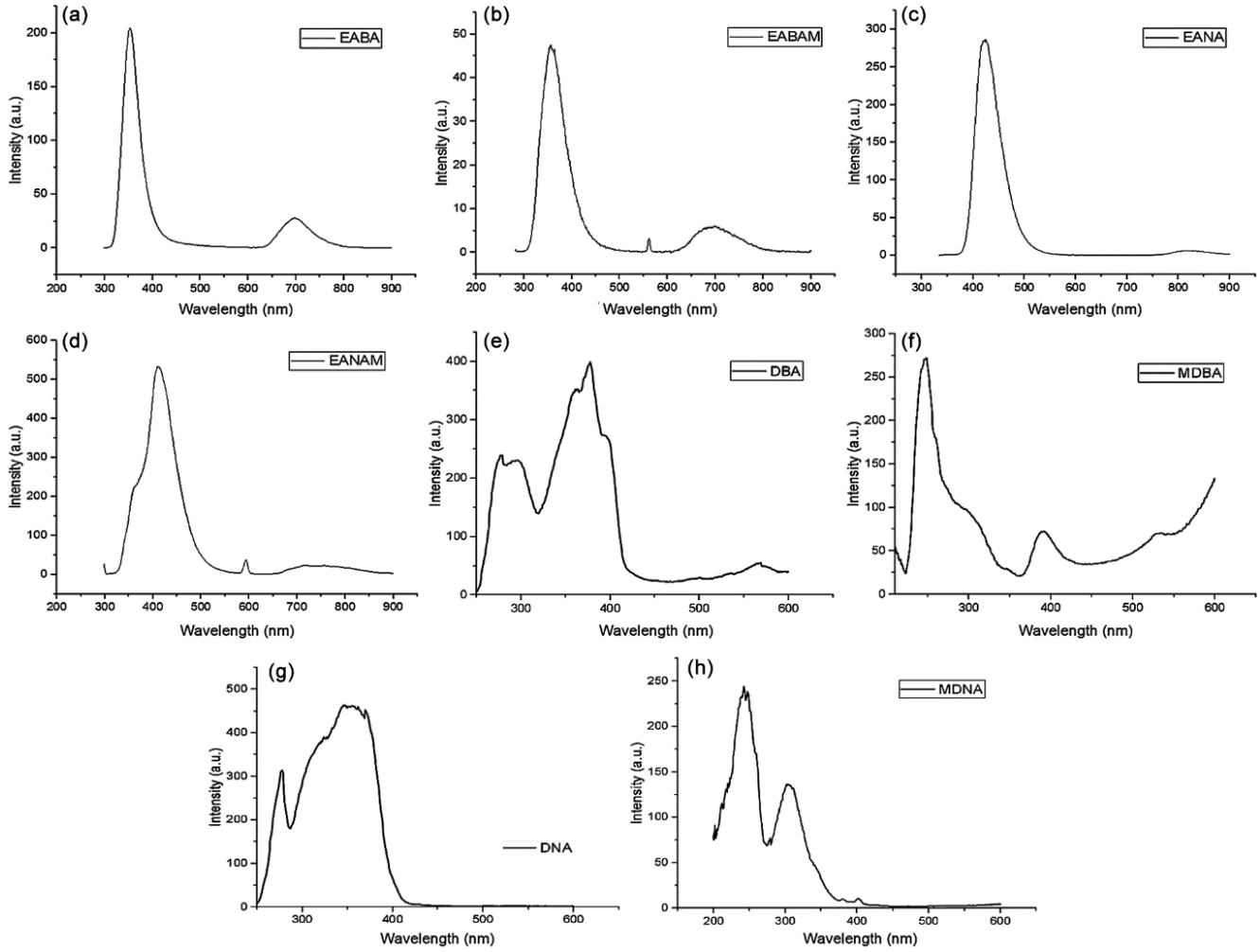

Fig. 7 — Emission Spectrum of ligands and complexes of EDTA and DTPA compounds

Manganese complexes of DTPA and EDTA with 4-amino benzoic acid and 6-amino naphthoic acid (Fig. 7) could be used in fluorescence imaging techniques. Further studies of this compound may also lead to imaging properties that can be used as contrast agents.

Anti-bacterial Activities

The Mn complexes showed good anti-microbial activity against various pathogens depending upon nature of the ligand in the complexes and concentration of the complexes. The zone of inhibition of the complexes and ligands is given in the table. Generally, it is suggested that the chelated complexes deactivate various cellular enzymes, which play a vital role in various metabolic pathways of these microorganisms. Other factors such as solubility, conductivity, and dipole moment, affected by the presence of metal ions, may also increase the biological activity of the metal complexes compared to the ligand[22]. These complexes may also disturb the respiration process of the cell and thus block the synthesis of proteins, which restricts further growth of the organism. All the ligands and complexes showed moderate activities towards the tested microbe *Staphylococcus aureus.*

The ligands and complexes of EDTA and DTPA with 4–amino benzoic acid and 6-amino naphthoic acid were tested against *Staphylococcus aureus,* a Gram positive bacteria, and *E. coli,* a Gram negative bacteria with the standards Ampicillin and Rifampicin at 20 µl concentration have been listed in Table 3. Considering the ligands of DTPA, 6-amino naphthoic acid with DTPA bis anhydride showed good activity against the bacteria. In EDTA ligands, 6-amino naphthoic acid showed good resistance against *Staphylococcus aureus,* and 4-aminobenzoic acid

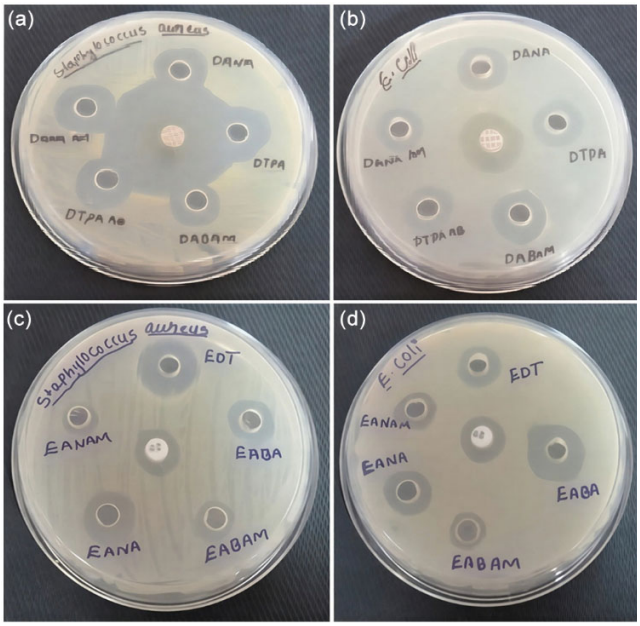

Fig. 8 — Zone of inhibition of ligands and complexes of DTPA and EDTA

Table 3 — Zone of inhibition of DTPA-based ligands and complexes

Sample	Zone of Inhibition (mm)	
	Staphylococcus aureus	*E. coli*
Standard (Rifampicin)	35	19
DTPABis	16	15
DTPABis-4ABA	16	16
DTPABis-6ANA	15	17
MnDTPABis-4ABA	16	15
MnDTPABis-6ANA	18	14
Standard (Ampicillin)	13	14
EDTABis	18	15
EDTABis-4ABA	13	18
EDTABis-6ANA	15	13
MnEDTABis-4ABA	9	10
MnEDTABis-6ANA	9	13

showed good resistance against *E. coli.* The complexes also showed considerable activity against the bacteria. In DTPA complexes, the complex of 4-amino benzoic acid showed good resistance to *E. coli.* In EDTA complexes, 6-amino naphthoic acid showed good activity against *E. coli* have been displayed in (Fig. 8). Also, to conclude further, it can be said that complexes of EDTA showed good bacterial-resistant activity than DTPA complexes.

Conclusions

Metal complexes of poly amino carboxylic acids were synthesized and subjected to various spectroscopic techniques. The ligands and complexes of EDTA and DTPA compounds showed good resistant activity against Gram positive bacteria *Staphylococcus aureus* and Gram negative bacteria *E. coli.* From the fluorescence spectrums of ligands and compounds, all the ligands and complexes showed good fluorescence activities with moderate and excellent emissions. These compounds may be further studied to utilize them for imaging techniques. Since the compounds also showed good biological activities, which were compatible with the human body, these compounds may also be studied further in usage as contrast agents in MRI imaging techniques.

Acknowledgements

The authors gratefully acknowledge the support of Avinashilingam Institute for Home Science and Higher Education for Women, Coimbatore, Tamil Nadu, India, for providing the experimental facilities essential for this research.

Conflicts of interest

All authors declare that they have no conflicts of interest.

Ethical approval

Not applicable.

Funding

This work was supported by the Seed Money Research Project Grants of Avinashilingam Institute for Home Science and Higher Education for Women, Coimbatore, Tamil Nadu, India. Project File No. Avinuty/Seed/SPSCS-2021-22/001; Dated: 25.03.2022.

Author contribution

Study conception and design: Amutha Selvi M. Data collection/ Experimental Work: Sivasankari J and Merlin Vinoliya Edwinraj. Analysis and interpretation of results: Amutha Selvi M and Merlin Vinoliya Edwinraj. Draft manuscript: Nandini B and Sivasankari J.

References

1 Hart J R, *Ullmann'sencyclopedia Industrial Chem*,(2000) https://doi.org/10.1002/14356007.a10_095.
2 DeBusk R, *Ethylenediaminetetraacetic acid (EDTA)*, University of Maryland Medical Center,2002.
3 Barett A J, *Methods in Enzymology*, (Elsevier, Ltd), 1995.
4 Paolieri M, *Bull Hist Chem*, 42(2017) 133.
5 Holleman A F & Wiberg E, *Inorganic Chemistry*, (Academic Press, San Diego), 2001.

6 Kálmán F K, Nagy V, Váradi B, Garda Z, Molnar E, Trencsenyi G & Tircsó G, *J Med Chem*, 63(2020) 6057.
7 Li X, Sun Y, Ma L, Liu G & Wang Z, *Molecules*, 25 (2020) 5072.
8 Kartamihardja A A P, Hanaoka H, Andriana P, Kameo S, Takahashi A, Koyama H & Tsushima Y, *British J Radiology*, 92 (2019) 20190062
9 Huang Y, Zhang X, Zhang Q, Dai X & Wu J, *Mag Reson Imaging*, 29 (2011) 554.
10 Li X, Sun Y, Ma L, Liu G & Wang Z, *Molecules*, 25 (2020) 5072.
11 Botta M, Carniato F, Esteban-Gómez D, Platas-Iglesias C & Tei L, *Fut Med Chem*, 11 (2019) 1461.
12 (a) Wai K, Chan Y, Barra S,Bottaand M, Wing T & Wong, *J Inorg Biochem*, 98 (2004) 677, ;(b) Gu S, Hee-K K, Lee G H, Kang Bong-S, Changand Y. & Tae-J K, *J Med Chem*, 54 (2011) 143, ;(c) Takács A, Napolitano R, Purgel M, Bényei A. C, Zékány L, Brücher E, Tóth I, Baranyai Z & Aime S, *Inorg Chem*, 53 (2014) 1858, ;(d) Jebasninghand B & Alexander V, *Inorg Chem*, 44 (2005) 9434.
13 http://casemed.case.edu/clerkships/neurology/NeurLrngObjectives/MRI.htm
14 Maiocchi A, *Mini Reviews Medic Chem*, 3(2003) 845.
15 Schmitt Willich H. (2007). *British J Radiology*, 80 (955) 581.
16 Major J L & Meade T J, *Accounts Chem Res*, 42 (2009) 893.
17 Runge, V. M, Dickey, K. M, Williams, N. M & Peng, X, *Investigative Radiology*, 37 (2002) 393.
18 Runge V M, Price A C, Wehr C J, Atkinson J B & Tweedle M F, *Investigative Radiology*, 20 (1985) 830.
19 Leydier A, Lin Y, Arrachart G, Turgis R, Lecerclé D, Favre-Reguillon A &Pellet Rostaing S, *Tetrahedron*,68 (2012) 1163.
20 Huang Y, Boamah P O, Gong J, Zhang Q, Hua M & Ye Y, *Carbohydrate Polymers*, 143 (2016) 288.
21 Huang Y, Cao J, Zhang Q, Lu Z R, Hua M Q, Zhang X Y & Gao H, *Magnetic Resonance Imaging*, 34 (2016) 1-7.
22 Al-Amiery A, Yasmein K, Al- Majeidy Abdulreazak H & Abood H, *Bioinorg Chem Appl*, 2011 (2011) 483101.
23 Gobika S & Suganthi A, *Int J Res Publication Rev*, 4 (2023) 5376.